FEDSM99-7916

THE EVOLUTION OF CAVITATION EVENTS WITH
SPEED AND SCALE OF THE FLOW

Tricia A. Waniewski[*]
Jet Propulsion Laboratory
California Institute of Technology
Pasadena, California 91109
Email: tricia.sur@jpl.nasa.gov

Christopher E. Brennen
Division of Engineering and Applied Science
California Institute of Technology
Pasadena, California 91125
Email: brennen@its.caltech.edu

ABSTRACT

This paper focuses on the different forms that individual cavitating events may take when the cavitation number is below the inception value (but not so low as to produce only attached cavities) and individual nuclei trigger individual cavitation events. It is a sequel to those of Kuhn de Chizelle *et al.* (1992a, 1992b, 1995) which described a set of cavitation scaling observations on simple Schiebe headforms conducted in the US Navy Large Cavitation Channel (LCC). The most common events observed in those experiments were traveling, hemi-spherical shaped bubbles which grew and collapsed as they were convected through the low pressure region on the headform. Several interesting variations were also observed, including the development of bubble tails and the triggering of patches, or local regions of attached cavitation. In the present paper, the frequency of occurrence of the various types of events is analyzed as well as how those probabilities changed with cavitation number, velocity and headform size. In general, the probabilities of tails and patches increased with decreasing cavitation number, but they also increased with increasing headform size and increasing velocity. A specific parametric dependence on these variables is suggested.

NOMENCLATURE

D Diameter of Schiebe headform
g Gravitational acceleration
p_v Vapor pressure
p_∞ Free stream pressure
Re Reynolds number, $\rho U D / \mu$
S Surface tension
U Free stream velocity
We Weber number, $\rho U^2 D / S$
μ Liquid dynamic viscosity
ρ Liquid density
σ Cavitation number, $2(p_\infty - p_v)/\rho U^2$

INTRODUCTION

Previous experimental studies of cavitating flows have demonstrated that the appearance of the cavitation events can change substantially with changes in the dimensions of the flow, in the flow velocity, and in the cavitation number (see, for example, Holl and Wislicenus, 1961). This paper focuses on these scale effects for the particular circumstances of traveling bubble cavitation. These effects alter the bubble growth and collapse processes and are important because they consequently affect the potential for cavitation damage and noise. Kuhn de Chizelle *et al.* (1992a, 1992b, 1995) performed experiments with cavitating flows over axisymmetric Schiebe headforms whose boundary layer does not separate in the low pressure region where cavitation occurs. They used the US Navy Large Cavitation Channel (LCC) facility to investigate these scaling effects. This paper documents the evolution of cavitation events with change in the speed and the scale of the flow using careful observation of the videotapes and other flow data taken from those experiments in the LCC.

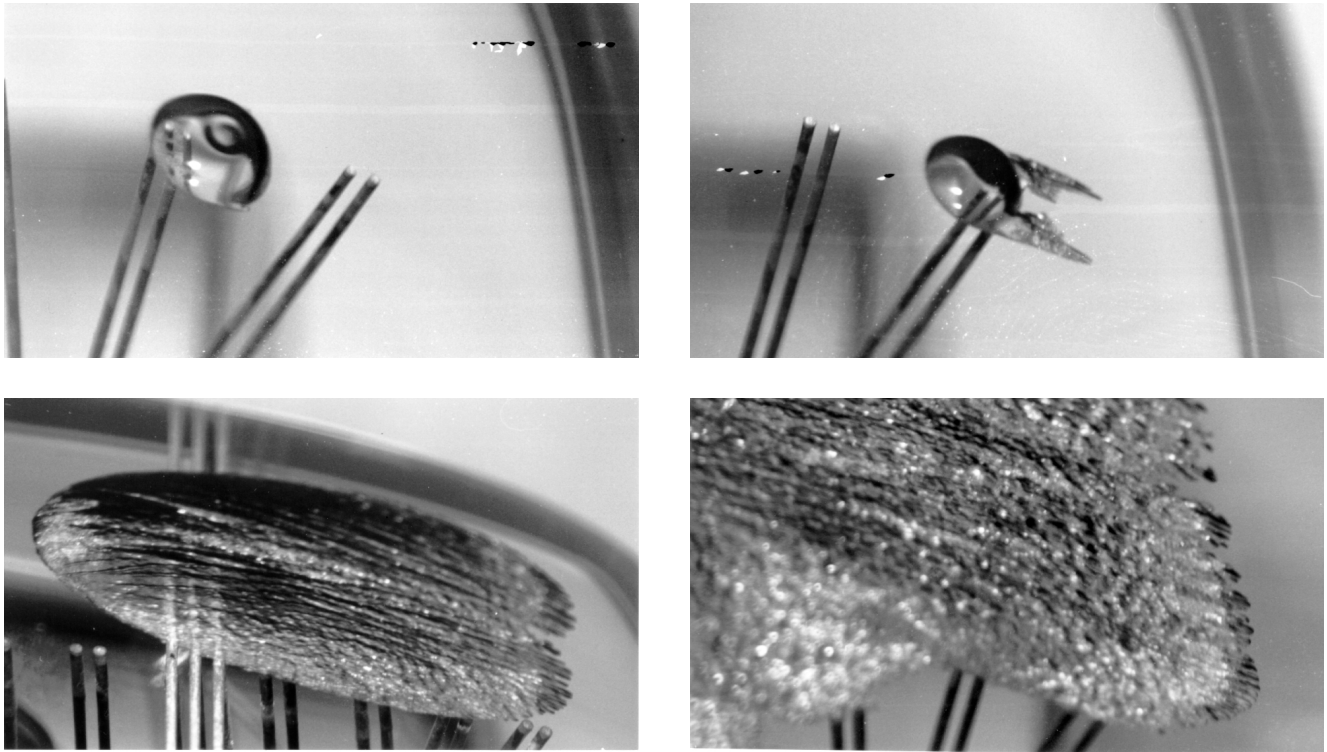[*] Address all correspondence to this author.

Figure 1. Photographs of various cavitation event types in the flow over a Schiebe headform at 30% dissolved oxygen content. The flow is from right to left and the distance between the electrodes is 2.54 cm. Top left: Spherical cap bubble with dimple for $D = 50.8$ cm at $U = 15$ m/s and $\sigma = 0.606$. Top right: Bubble with attached tails for $D = 50.8$ cm at $U = 15$ m/s and $\sigma = 0.606$. Lower left: Patch cavitation for $D = 25.4$ cm at $U = 15$ m/s and $\sigma = 0.530$. Lower right: Extensive attached cavitation for $D = 50.8$ cm at $U = 15$ m/s and $\sigma = 0.537$.

OBSERVATIONS OF CAVITATING FLOWS

Flows over Schiebe headforms having diameters, D, of 5.08 cm, 25.4 cm and 50.8 cm were investigated at velocities, U, of 9 m/s, 11.5 m/s, and 15 m/s, dissolved oxygen contents of 30% and 80%, and at a variety of cavitation numbers, σ, between 0.420 and 0.779 (Kuhn de Chizelle *et al.*,1992a, 1992b, 1995). For each flow condition, the available photographs and videotapes were carefully studied. It was determined that the cavitation events could be classified into the following four categories: spherical cap bubbles, bubbles with attached tails, patches, and extensive attached cavitation. Figure 1 depicts a typical example of a cavitation event in each of these categories. Holl and Carroll (1979) describe similar types of cavitation events in flows over Schiebe headforms under similar flow conditions. Huang (1979) also observed a variety of types of events during similar experiments.

The spherical cap bubbles were the most common type of cavitation event and a photograph of such a bubble is included in figure 1, upper left. These bubbles are generally hemispherical in shape and, like the one in figure 1, many have a visible indentation or dimple on their outer aspect. The calculations of Kuhn de Chizelle *et al.* (1995) exhibit vestiges of a similar dimple which seems to be caused by the large pressure gradients nor-mal to the headform surface. Previously published photographs capture these bubbles in various stages of growth and collapse. A detailed description of the typical bubble evolution is presented by Ceccio and Brennen (1991).

The second most common cavitation event was a bubble with attached tails as shown in figure 1 upper right and described by Ceccio and Brennen (1991). The tails, located in the wake of the bubble, are cavitating, trailing vortices triggered by the passage of the traveling bubble. The ends of the tails are attached to the surface of the headform and to the lateral extremities of the bubble. They grow in size as the bubble continues to travel downstream, persisting even after the main bubble has collapsed. These tails can be explained as follows. As the bubble interacts with the boundary layer it acquires circulation; consequently vortex lines emanate from the sides of the bubble (like wing-tip vortices) and must terminate at some point on the headform surface behind the bubble. Such vortices will always be present, but only when they are strong enough will the pressure in the core be sufficiently low for the core to fill with vapor. Note that the formation of vapor-filled cores also could be caused by ventilation from the main bubble. In either case, the vapor-filled cores become visible as "tails".

2

The cavitation patches similarly were triggered by a single bubble traveling over the headform; an example is shown in figure 1, lower left. They occur when a passing bubble triggers a separated region in its wake, and this separated region fills with vapor. In this respect they are a natural inward extension of the tails. The upstream end of the attached cavitation patch thus formed is located on the headform surface and the downstream end is extended by the passage of the now-distorted bubble. The patches often would persist for a period of time significantly longer than the time required for passage of the bubble. The patches as well as the attached tails had a rough, turbulent surface as seen in figure 1, lower left. When a multitude of patches occurred, the cavitation evolved into extensive attached cavitation as shown in figure 1, lower right.

All of the cavitation types could occur either simultaneously or separately. For example, when there was extensive attached cavitation over the headform, distinct spherical cap bubbles remained easily observable. Sometimes they would ride up and over an attached cavity as described by Kuhn de Chizelle *et al.* (1995) and by Li and Ceccio (1994).

For each of the 32 flow conditions recorded on the videotape, 100 individual frames were carefully analyzed. The cavitation events were counted and classified into the categories described above. Since only one quarter of the headform was visible, these numbers were multiplied by four to account for the entire surface of the headform and then averaged over all 100 frames. Difficulties were encountered in counting cavitation events in some cases because of the large number of observable bubbles in the incoming flow. In addition, difficulties were experienced in counting the number of patches and bubbles with attached tails in flow conditions that exhibited extensive attached cavitation; consequently, the event statistics under these circumstances are less reliable.

CAVITATION EVENT STATISTICS

Figure 2 illustrates the variation of the average number of observable events on the headform with cavitation number for the different flow conditions. Several important trends are evident. First, it is apparent for all the operating conditions shown, that as the cavitation number decreases, the total number of cavitation events on the headform increases since a larger number of nuclei are activated at lower cavitation numbers (Brennen, 1995). Second, as the headform size increases, the total number of cavitation events on the headform increases due to geometric effects. The larger the headform, the more cavitation nuclei pass through the low pressure region on the headform; therefore, it is more likely for a cavitation event to occur. Note, however, that the difference between the 25.4 cm headform data and that for the 50.8 cm headform is somewhat greater than a factor of four. Third, as the flow velocity increases, the total number of cavitation events on the headform decreases. This is probably due to the fact that, for a given cavitation number, the pressure, p_∞, will be lower as the ve-
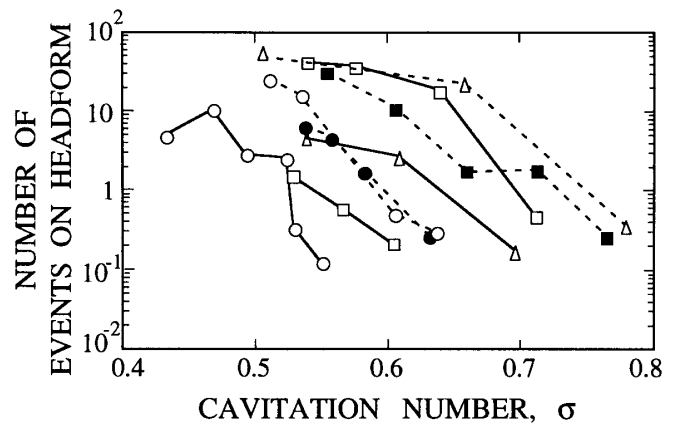

Figure 2. The average number of observable events on the headform as a function of cavitation number at 30% dissolved oxygen content: ($\triangle$) for U = 9 m/s, ($\square$) for U = 11.5 m/s, and ($\odot$) for U = 15 m/s; (—) for D = 25.4 cm, and ($\cdots$) for D = 50.8 cm. The filled symbols represent a dissolved oxygen content of 80%.

locity is decreased and will cause an increase in the nuclei population in the water tunnel facility (Kuhn de Chizelle *et al.*, 1995; Liu and Brennen, 1998). Finally, figure 2 demonstrates that, as the air content of the water is increased, the total number of cavitation events on the headform only undergoes minor changes. More information on the relation between the nuclei population and the dissolved oxygen content would be needed to understand this last result.

The flow conditions were then separated according to headform diameter, flow velocity, and air content and the variation in the types of cavitation events were studied as a function of cavitation number. Figure 3 is a typical result and shows the data for the 50.8 cm diameter headform with U = 11.5 m/s and 30% dissolved oxygen content. Note that dashed lines denote conditions for which extensive attached cavitation occurred. Under these conditions, the specific types of cavitation events, especially bubbles with attached tails and patches, could not be reliably counted. However, it was possible to count the spherical cap bubbles riding above the attached cavities. Error bars which represent ±0.2 standard deviations are displayed in figure 3, except in the cases where the mean minus 0.2 standard deviations is a negative number; for these cases only +0.2 standard deviations is shown. Much of the data is positively skewed, or the mean is greater than the median.

Figure 4 displays the results from the 25.4 cm diameter headform at 30% dissolved oxygen content for different velocities. The graphs present the number of cavitation events as a function of cavitation number and the error bars, similar to those of figure 3, are omitted for clarity. At U = 9 m/s, spherical cap bubbles account for most of the cavitation events. However, at U = 11.5 m/s a greater percentage of bubbles with attached tails and
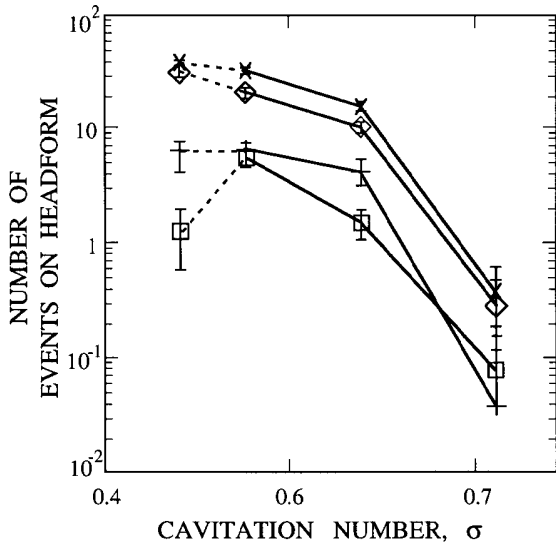
Figure 3. The average number of observable events as a function of cavitation number for 50.8 cm diameter headform at 30% dissolved oxygen content, and $U = 11.5$ m/s. Data is shown for the number of spherical cap bubbles (⊶), for the number of bubbles having attached tails (⊢⊞⊣), for the number of patches (⊢⊟⊣), and for the number of total cavitation events (⊢×⊣) on the headform. The error bars represent ± 0.2 standard deviations.

patches are present, and at $U = 15$ m/s the patches are the dominant form of cavitation event with attached tails being the most infrequent. Figure 5 presents the percentage of the observed events with tails and with patches for the two larger headforms and the two larger tunnel velocities as a function of cavitation number. The remainder of the events were traveling bubbles without tails. Though the data is scattered, several trends can be perceived. As the cavitation number decreases below about 0.6, the chance of a traveling bubble developing tails increases. It is not clear how the chance of tails varies with headform diameter, D, or tunnel velocity, U, but the chance of patches does seem to increase notably with increasing velocity. A similar set of graphs was produced for the 25.4 cm diameter headform with 80% dissolved air content and also for the 50.8 cm diameter headform with 30% dissolved air content.

To examine these trends further, consider the typical forces causing bubble distortion into tails or patches and those resisting distortion. The typical laminar boundary layer shear stress acting on a traveling bubble is given roughly by $(\rho\mu U^3/D)^{\frac{1}{2}}$ and the typical surface tension stress resisting distortion is S/D. The ratio of these stresses suggests that the likelihood of tail or patch formation increases with $\rho\mu U^3 D/S^2$ or We^2/Re where the Weber number, $We = \rho U^2 D/S$, and the Reynolds number, $Re = \rho U D/\mu$. Accordingly, the percentage of events with tails and of events with patches are plotted against We^2/Re in figure 6. The lower graph strongly suggests an onset of patch formation about $We^2/Re =$
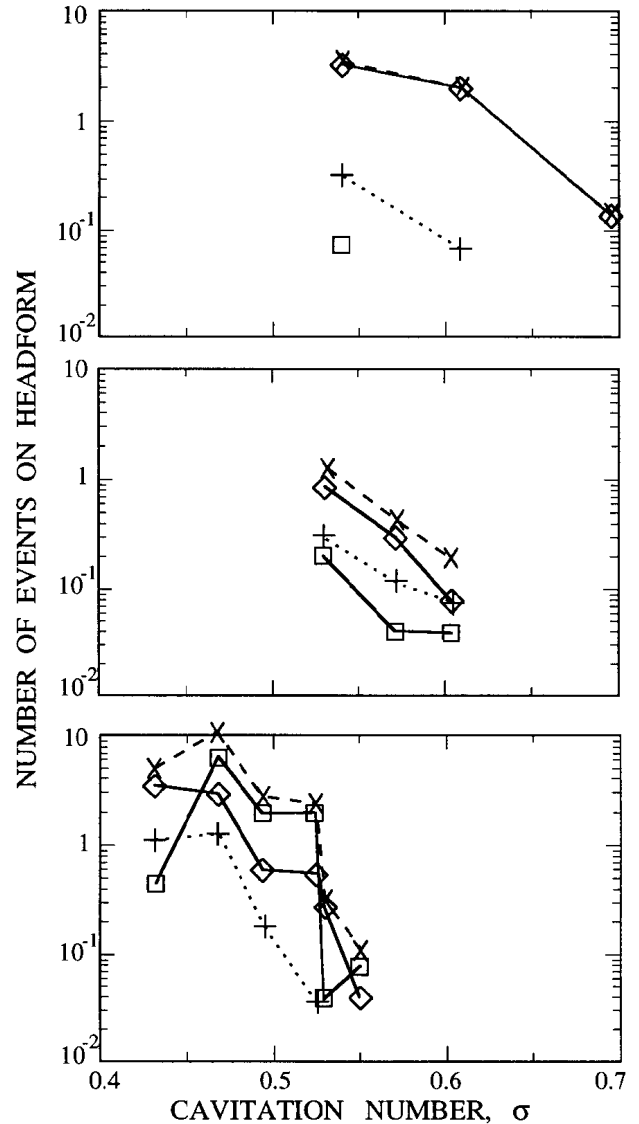

Figure 4. The average number of observable events as a function of cavitation number for the 25.4 cm diameter headform at a dissolved oxygen content of 30% for three velocities. Data is shown for the number of spherical cap bubbles ($\diamond$), for the number of bubbles having attached tails ($+$), for the number of patches ($\square$), and for the number of total cavitation events ($\times$) on the headform. Top: $U = 9.0$ m/s. Middle: $U = 11.5$ m/s. Bottom: $U = 15.0$ m/s.

10^6. The upper graph is less compelling, but it seems to indicate an onset of tails at a lower value of We^2/Re.

CONCLUSIONS

The focus of this paper is on the different forms which individual cavitating events may take. When the cavitation number
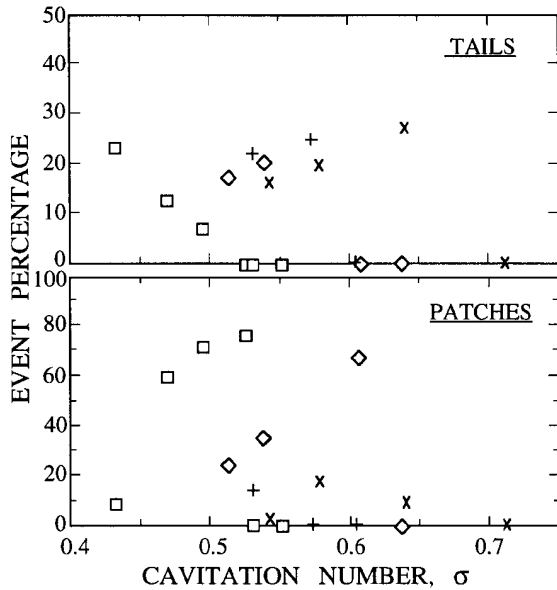
4

Figure 5. The percentage of events in the form of tails (upper graph) and patches (lower graph) as a function of cavitation number: for $D = 25.4$ cm, $U = 15$ m/s ($\square$); for $D = 50.8$ cm, $U = 15$ m/s ($\diamond$); for $D = 25.4$ cm, $U = 11.5$ m/s ($+$); and for $D = 50.8$ cm, $U = 11.5$ m/s ($\times$).
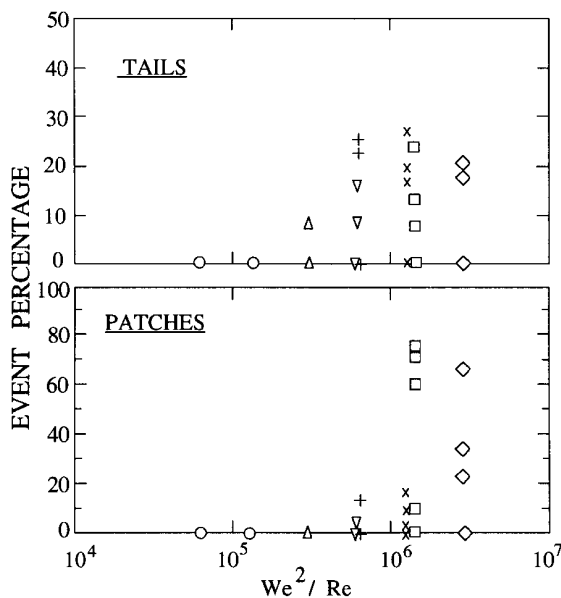

Figure 6. The percentage of events in the form of tails (upper graph) and patches (lower graph) as a function of We^2/Re: for $D = 2.54$ cm ($\circ$); for $D = 25.4$ cm, $U = 15$ m/s ($\square$), $U = 11.5$ m/s ($+$) and $U = 9$ m/s ($\triangle$); for $D = 50.8$ cm, $U = 15$ m/s ($\diamond$), $U = 11.5$ m/s ($\times$) and $U = 9$ m/s ($\triangledown$).

is below the inception value (but not so low as to produce only attached cavities) individual nuclei trigger individual cavitation events. The most common events observed in these experiments are traveling, hemi-spherical bubbles which grow and collapse as they are convected through the low pressure region of the headform. However, as previously observed by Kuhn de Chizelle *et al.* (1992a, 1992b), several interesting variations may occur, including the development of bubble tails and the triggering of a patch, or local region of attached cavitation. In the present paper, the frequency of occurrence of these various types of cavitation events is documented and the change in their probabilities with cavitation number, velocity and headform size is explored. In general, the probabilities of tails and patches increase with decreasing cavitation number; however, they also increase with increasing scale of the flow and increasing velocity. The present paper suggests a specific parametric dependence on size and velocity.

The damage and noise produced by the cavitation probably depends on the type of event (Ceccio and Brennen, 1991; Kuhn de Chizelle *et al.*, 1995); therefore, understanding how noise and damage scale requires an understanding of how the event probablities scale. This study revealed a number of scaling effects in cavitating flows over headforms. First, as the cavitation number increases, the total number of cavitation events on the headform decreases since a larger number of nuclei are activated at lower cavitation numbers. Second, as the headform diameter increases, the total number of cavitation events on the headform increases. Clearly, this can be attributed to geometric reasons since more nuclei pass through the low pressure region on a larger headform. Third, as the flow velocity decreases, the total number of cavitation events on the headform increases. This is probably because, for a given cavitation number, the pressure, p_∞, will be lower as the velocity is decreased and will cause an increase in the nuclei population. Fourth, as the air content of the water increased, the total number of cavitation events on the headform only exhibited modest increases.

ACKNOWLEDGEMENTS

REFERENCES

Ceccio, S.L. and Brennen, C.E., 1991, "Observations of the dynamics and acoustics of travelling bubble cavitation", *J. Fluid Mech.*, Vol. 233, pp. 633–660.

Holl, J.W. and Wislicenus, G.F., 1961, "Scale effects on cavitation", *ASME J. Basic Eng.*, Vol. 83, pp. 385–398.

Holl, J.W. and Carroll, J.A., 1979, "Observations of the various types of limited cavitation on axisymmetric bodies", *Proc. ASME Int. Symp. on Cavitation Inception*, pp. 87–99.

Huang, T.T., 1979, "Cavitation inception observations on six axisymmetric headforms", *Proc. ASME Int. Symp. on Cavitation Inception*, pp. 51–61.

Kuhn de Chizelle, Y., Ceccio, S.L., Brennen, C.E. and Gowing, S., 1992a, "Scaling experiments on the dynamics and acoustics of travelling bubble cavitation", *Proc. 3rd I.Mech.E. Int. Conf. on Cavitation, Cambridge, England*, pp. 165–170.

Kuhn de Chizelle, Y., Ceccio, S.L., Brennen, C.E. and Shen, Y., 1992b, "Cavitation scaling experiments with headforms: bubble acoustics", *Proc. 19th Symp. on Naval Hydrodynamics, Seoul, Korea*, pp. 72–84.

Kuhn de Chizelle, Y., Ceccio, S.L. and Brennen, C.E., 1995, "Observations, scaling and modelling of travelling bubble cavitation", *J. Fluid Mech.*, Vol. 293, pp. 99–126.

Liu, Z., Kuhn de Chizelle, Y. and Brennen, C.E., 1993, "Cavitation event rates and nuclei distributions", *Proc. ASME Symp. on Cavitation Inception*, Vol. FED-177, pp. 13–24.

Li, C. and Ceccio, S.L., 1994, "Observations of the interaction of cavitation bubbles with attached cavities", *Proc. ASME Symp. on Cavitation and Gas-Liquid Flows in Fluid Machinery and Devices*, Vol. FED-190, pp. 283–289.